Enhanced plasmon anomaly in the dynamical conductivity of heterostructures with large spacer

A. Gold
Department of Physics, Massachusetts Institute of Technology, Cambridge, Massachusetts 02139
(Received 14 August 1989)

We calculate the frequency-dependent scattering rate $M''(\omega)$, which determines the dynamical conductivity of a disordered two-dimensional electron gas. The existence of plasmons in an interacting electron gas gives rise to a strongly frequency-dependent scattering rate. For $Al_xGa_{1-x}As/GaAs$ heterostructures with large spacer width α, we get an analytical result for the scattering rate: $M''(\omega)=M''(0)[1+A|\omega|^5\exp(-B\omega^2)]$. The coefficients A and B depend on the Fermi wave number k_F, the effective Bohr radius a^*, and α. $M''(\omega)$ peaks at $\omega_0=\varepsilon_F(5a^*/\alpha)^{1/2}/(k_Fa^*)$, where ε_F is the Fermi energy. The high-frequency scattering rate is also calculated: $M''(\omega\gg 2\varepsilon_F)\ll M''(0)$. We predict a maximum linewidth for plasmons with wave number $q_0=5/(4\alpha)$. The relevance of our theory to anomalies found in cyclotron-resonance experiments is discussed.

I. INTRODUCTION

Two-dimensional electron systems can be used to study interacting electrons at low temperatures (for a review, see Ref. 1). Strong anomalies have been found in cyclotron-resonance experiments in silicon metal-oxide-semiconductor (MOS) structures.[2] It was claimed that novel phenomena have been observed in experiments on the dynamical conductivity of two-dimensional electrons at finite magnetic field. A Wigner crystal was discussed in connection with data on silicon MOS structures.[3] Exciton physics[4] has been related to some experimental results on $Al_xGa_{1-x}As/GaAs$ heterostructures.[5] In this paper, I will present arguments which bring into question the theoretical interpretation of the experimental data as given in Refs. 3 and 5.

Plasmon-density excitations are the most important concept of the long-range Coulomb repulsion of interacting electrons.[6] Anomalous linewidths and energy shifts of plasmons in silicon MOS structures have been reported.[7] An anomalous enhancement of the dynamical conductivity at finite frequency in the same structure was interpreted as a result of plasmon dynamics.[8] Theoretical studies of the dynamical conductivity for disordered interacting electrons in silicon MOS structures showed that the scattering rate is strongly frequency dependent.[9] The anomalies found in plasmon-resonance experiments[7] have been explained by this frequency-dependent scattering time.[9,10]

The existence of plasmons in an interacting-electron gas enhances the density of final states for the decay rate of the current. Therefore, the frequency-dependent current relaxation rate is enhanced in comparison to the static value. In silicon MOS structures with impurities at the Si/SiO_2 interface the enhancement factor is about 3.[9,10] In the calculations of the dynamical conductivity of $Al_xGa_{1-x}As/GaAs$ heterostructures with a spacer width $\alpha=150$ Å the enhancement factor was about 5.[11]

The theoretical results on silicon MOS structures[9,10] and $Al_xGa_{1-x}As/GaAs$ heterostructures[11] were given as numerical results. Therefore, it is difficult for experimentalists to compare quantitatively with the theory. In this paper, I present analytical results for $Al_xGa_{1-x}As/GaAs$ heterostructures with large spacer widths. Plasmons in $Al_xGa_{1-x}As/GaAs$ heterostructures have been studied recently.[12-15] I shall argue that the frequency-dependent scattering time is most easily studied by plasmon-resonance experiments. I propose some experiments to test the theoretical predictions of my theory. Furthermore, I analyze some experimental results found for the cyclotron resonance in these structures[5,16] by neglecting the effects of the magnetic field on the scattering rate. The agreement between theory and experiments is surprisingly good.

The paper is organized as follows. In Sec. II the model and the theory are described. The results for large spacer are presented in Sec. III. Finite-width effects of the doping and the electron gas are calculated in Sec. IV. Other scattering mechanisms are discussed in Sec. V. The application to the plasmon resonance and the cyclotron resonance is presented in Sec. VI. The discussion of the results is given in Sec. VII. I compare my results with experimental results in Sec. VIII. The conclusion is in Sec. IX.

II. MODEL AND THEORY

A. Model

I consider a two-dimensional interacting-electron gas disordered by a sheet of charged impurities with impurity density N_i. The impurities are separated from the electron gas by a spacer of width α. The width of the doping layer is δ. $1/b$ is the extension parameter of the electron gas perpendicular to the $Al_xGa_{1-x}As/GaAs$ interface. The Fourier transform of the random potential $\langle|U(\mathbf{q})|^2\rangle$ is written as[11]

$$\langle|U(\mathbf{q})|^2\rangle=N_i\left[\frac{2\pi e^2}{\epsilon_L q}\right]^2 e^{-2q\alpha}\frac{1-e^{-2q\delta}}{2q\delta}\frac{1}{(1+q/b)^6}\ . \tag{1a}$$

ϵ_L is the background dielectric constant and q the wave number. The extension parameter b is expressed in terms of the electron density N and the depletion density N_D. For $Al_xGa_{1-x}As/GaAs$ heterostructures one finds[1]

$$ba^*=3.73[N(a^*)^2+32N_D(a^*)^2/11]^{1/3} . \quad (1b)$$

a^* is the effective Bohr radius: $a^*=\epsilon_L\hbar^2/me^2\sim 100$ Å. $m=0.067m_e$ is the electron mass in the lattice. m_e is the vacuum electron mass. In the following, I use $\hbar=1$ unless specified otherwise. As mentioned before, the main result of the long-range Coulomb interaction is the existence of a plasmon branch with plasmon dispersion $\omega_{p0}(q)$:

$$\omega_{p0}(q)^2=4g_v\left[\frac{\varepsilon_F}{k_Fa^*}\right]^2(qa^*) , \quad (2)$$

where g_v is the valley degeneracy, ε_F is the Fermi energy, and k_F is the Fermi wave number. Equation (2) describes the plasmon dispersion for small q. For large q, additional terms must be taken into account,[1] see Sec. VII A.

B. Theory

I calculate the dynamical conductivity for zero temperature. The disorder in the system gives rise to a finite conductivity. I express the dynamical conductivity $\sigma(z)$ for complex frequency z as[17]

$$\sigma(z)=\frac{Ne^2}{m}\frac{i}{z+M(z)} . \quad (3)$$

$M(z)$ is the current relaxation kernel with a real (reactive) part and an imaginary (dissipative) part,

$$M(\omega+i0)=M'(\omega)+iM''(\omega) . \quad (4)$$

$1/M''(\omega)=\tau(\omega)$ is the frequency-dependent relaxation time.

The main reason for the frequency dependence of the current relaxation kernel is the decay of current modes into plasmon modes. The other decay channel, the decay of current modes into particle-hole excitations, is weakly frequency dependent for $\omega<2\varepsilon_F$. The high-frequency expression is specified later. Therefore, I rewrite Eq. (4) as

$$M(\omega+i0)=M_p'(\omega)+i[M''(0)+M_p''(\omega)] , \quad (5)$$

and p indicates the plasmon channel. Following previous work,[9] I write

$$\left.\begin{matrix}M_p'(\omega)\\M_p''(\omega)\end{matrix}\right\}=\frac{1}{4\pi Nm}\int_0^\infty dq\, q^3\langle|U(\mathbf{q})|^2\rangle\times\begin{Bmatrix}\phi_p'(q,\omega)\\\phi_p''(q,\omega)\end{Bmatrix} . \quad (6)$$

$\phi_p(q,\omega+i0)=\phi_p'(q,\omega)+i\phi_p''(q,\omega)$ is the density-density correlation function in the plasmon-pole approximation. Explicitly one gets[9]

$$\phi_p'(q,\omega)=\frac{-\omega g_I(q)}{\omega^2-\omega_{p0}(q)^2} \quad (7a)$$

and

$$\phi_p''(q,\omega)=\tfrac{1}{2}\pi g_I(q)[\delta(\omega-\omega_{p0}(q))+\delta(\omega+\omega_{p0}(q))] . \quad (7b)$$

$g_I(q)$ is the compressibility of the interacting-electron gas. I use $g_I(q)$ for small q given by

$$g_I(q)=\frac{1}{V(q)}=\frac{\epsilon_Lq}{2\pi e^2} . \quad (8)$$

$V(q)$ is the electron-electron interaction potential.

C. The high-frequency conductivity

In Eq. (5), I neglected the frequency dependence of the particle-hole decay channel. However, for very large frequencies the inverse scattering time is determined by the frequency dependence of the particle-hole channel and is expressed as

$$M''(\omega\gg2\varepsilon_F)=\frac{1}{4\pi Nm}\int_0^\infty dq\, q^3\langle|U(\mathbf{q})|^2\rangle\phi_0''(q,\omega) . \quad (9)$$

$\phi_0''(q,\omega)$ is the density-density correlation function of the non-interacting-electron gas. $\phi_0''(q,\omega)$ is finite for $q_1<q<q_2$ with $q_1=(k_F^2+2m\omega)^{1/2}-k_F$ and $q_2=(k_F^2+2m\omega)^{1/2}+k_F$. For the calculation of the q integral in Eq. (9), I use

$$\int_{q_1}^{q_2}dq\, q\phi_0''(q,\omega)=\phi_0''(q^*,\omega)\int_{q_1}^{q_2}dq\, q , \quad (10a)$$

and with the f-sum rule,[6] I get for q^*

$$\frac{(q^*)^2}{2m}=\omega\left[1+\frac{2\varepsilon_F}{\omega}\right] . \quad (10b)$$

The explicit calculation of $\phi_0''(q^*,\omega)$ for $\omega\gg2\varepsilon_F$ gives

$$\phi_0''(q^*,\omega)=N\left[\frac{1}{\varepsilon_F|\omega|^3}\right]^{1/2} . \quad (11)$$

With Eqs. (1) and (9)–(11), I get for remote impurity doping

$$M''(\omega\gg2\varepsilon_F)=4g_v\varepsilon_F\frac{N_i}{N}\frac{1}{(a^*k_F)^2(\delta k_F)}\left[\frac{\varepsilon_F}{\omega}\right]^{3/2}e^{-2k_F\alpha(\omega/\varepsilon_F)^{1/2}}(1-e^{-2k_F\delta(\omega/\varepsilon_F)^{1/2}})\frac{1}{[1+(\omega/\varepsilon_F)^{1/2}k_F/b]^6} . \quad (12)$$

Equation (12) clearly shows that the large-q behavior of the random potential determines the high-frequency dependence of the scattering rate of the electron-hole channel.

III. RESULTS FOR $\delta=0$ AND $1/b=0$

In this section, I discuss the random potential with $\delta=0$ and $1/b=0$. Detailed analytical results are derived.

A. The scattering rate

In the following, I present the analytical results for $M_p'(\omega)$ and $M_p''(\omega)$ and discuss the relevant frequency scales which define the structures seen in $M_p'(\omega)$ and $M_p''(\omega)$. The magnitude of $M_p'(\omega)$ and $M_p''(\omega)$ is defined by the relaxation rate for zero frequency $M''(\omega=0)$, expressed as[18,19]

$$M''(\omega=0)=\varepsilon_F\frac{1}{g_v}\frac{N_i}{N}\frac{1}{(2k_F\alpha)^3}\ . \tag{13}$$

With Eqs. (1), (2), (6)–(8), and (13), I get

$$M'(\Omega)=M''(\omega=0)\left[2g_v\frac{\alpha}{a^*}\right]^{1/2}\times\Omega[1+\Omega^2-\Omega^4\mathrm{Ei}(\Omega^2)e^{-\Omega^2}] \tag{14a}$$

and

$$M''(\Omega)=M''(\omega=0)\left[1+\pi\left[2g_v\frac{\alpha}{a^*}\right]^{1/2}|\Omega|^5e^{-\Omega^2}\right]\ . \tag{14b}$$

$\mathrm{Ei}(x)$ is the exponential-integral function.[20] In Eq. (14), I introduced a normalized frequency Ω, defined as

$$\Omega=\frac{\omega}{\varepsilon_F}\left[\frac{1}{2g_v}\alpha a^*k_F^2\right]^{1/2}\ . \tag{15}$$

$M''(\omega)$ versus ω is shown in Fig. 1 for $N=1.5\times10^{11}$ cm^{-2} and $\alpha=750$ Å. A pronounced maximum ($dM_p''/d\omega=0$) is found for $\omega=\omega_0$. From Eq. (14b), one gets

$$\omega_0=\varepsilon_F\frac{1}{k_Fa^*}\left[5g_v\frac{a^*}{\alpha}\right]^{1/2}=\frac{e^2}{\epsilon_L}N^{1/2}\left[\frac{5\pi a^*}{2\alpha}\right]^{1/2}\ . \tag{16}$$

Due to the plasmon dynamics, the scattering rate is strongly enhanced for finite frequency. The enhancement factor at ω_0 is written as

$$M_p''(\omega_0)/M''(\omega=0)=\pi\left[g_v\frac{5^5\alpha}{2^4a^*}\right]^{1/2}e^{-5/2}=3.60\left[g_v\frac{\alpha}{a^*}\right]^{1/2}\ . \tag{17a}$$

The enhancement factor in Fig. 1 is about 10, which is much larger than the enhancement found in silicon MOS systems.[9] The real part of $M(\omega)$ at ω_0 is expressed as

$$M'(\omega_0)/M''(\omega=0)=-0.29\left[g_v\frac{\alpha}{a^*}\right]^{1/2}\ . \tag{17b}$$

The width of the maximum of $M''(\omega)$ is estimated by the frequencies $\omega_{1,2}$, which are defined by $d^2M_p''/d^2\omega=0$, and given by

$$\omega_{1,2}=\omega_0\{[11\pm(41)^{1/2}]/10\}^{1/2}\ . \tag{18a}$$

Explicitly, I get $\omega_1=0.68\omega_0$ and $\omega_2=1.32\omega_0$. The width of the resonance is defined as

$$\omega_2-\omega_1=0.64\omega_0\ . \tag{18b}$$

ω_0, ω_1, and ω_2 are indicated in Fig. 1.

$M'(\omega)$ versus ω is shown in Fig. 2 for the same parameters as for Fig. 1. $M'(\omega)$ changes sign at ω^*, where $M'(\omega^*)=0$. $M'(\omega)$ shows a maximum at ω_- and a minimum at ω_+. Using Eq. (14a), I obtain the following numerical values:

$$\omega^*=0.97\omega_0\ , \tag{19a}$$

$$\omega_-=0.63\omega_0\ , \tag{19b}$$

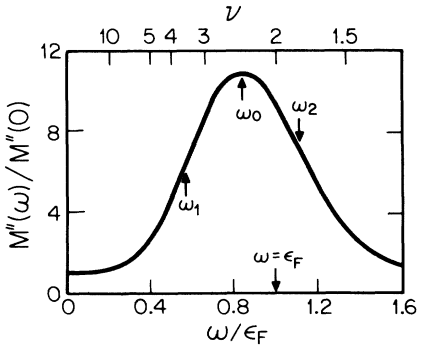

FIG. 1. $M''(\omega)$ vs frequency ω for $N=1.5\times10^{11}$ cm^{-2} and $\alpha=750$ Å according to Eq. (14b). ω_0, ω_1, and ω_2 are discussed in the text, see Eqs. (16) and (18a). ε_F if the Fermi energy. ν is the Landau filling factor defined by $\nu=2\varepsilon_F/\omega$ ($g_v=1$).

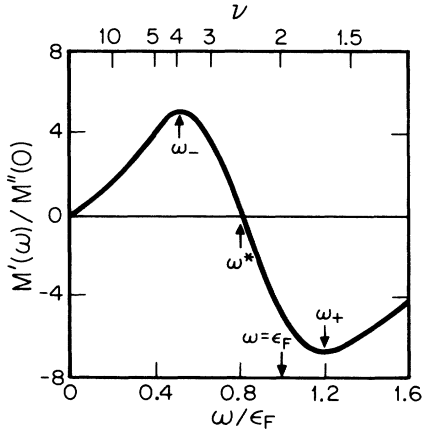

FIG. 2. $M'(\omega)$ vs frequency ω for $N=1.5\times10^{11}$ cm^{-2} and $\alpha=750$ Å according to Eq. (14a). ω^*, ω_+, and ω_- are discussed in the text, see Eq. (19). ε_F is the Fermi energy. ν is the Landau filling factor defined by $\nu=2\varepsilon_F/\omega$ ($g_v=1$).

$$\omega_+ = 1.43\omega_0 \ , \tag{19c}$$

which lead to

$$M'(\omega_-)/M''(\omega=0) = +1.84 \left[g_v \frac{\alpha}{a^*} \right]^{1/2} \tag{20a}$$

and

$$M'(\omega_+)/M''(\omega=0) = -2.44 \left[g_v \frac{\alpha}{a^*} \right]^{1/2} . \tag{20b}$$

The range of $M'(\omega)$ is expressed as

$$[M'(\omega_-) - M'(\omega_+)]/M''(\omega=0) = 4.28 \left[g_v \frac{\alpha}{a^*} \right]^{1/2} . \tag{21}$$

Comparing Eq. (17a) with Eq. (21), I remark that the variations of $M'(\omega)$ and $M''(\omega)$ are of same order of magnitude.

B. The plasmon anomaly in the conductivity

In the case of $\omega \gg |M'(\omega)|, M''(\omega)$ (for small N_i) the dynamical conductivity can be written as $\sigma'(\omega) = Ne^2 M''(\omega)/(m\omega^2)$ and the frequency dependence of the conductivity is determined by $M''(\omega)$. Then one expects two peaks for the frequency-dependent conductivity: The first peak at $\omega=0$ is the Drude peak of Lorentz form with width $M''(\omega=0)$. The second peak at $\omega=\omega_{0\sigma}=\omega_0(\frac{3}{5})^{1/2}$ is non-Lorentzian and much broader than the peak at $\omega=0$. For $\omega=\omega_{0\sigma}$, I get

$$\sigma'(\omega_{0\sigma}) = \frac{e^2}{h} \frac{1}{6g_v} \frac{N_i}{N} \frac{1}{2k_F\alpha} \frac{a^*}{\alpha} \left[1 + 2.73 \left[g_v \frac{\alpha}{a^*} \right]^{1/2} \right] . \tag{22}$$

The peak conductivity at $\omega_{0\sigma}$ depends on α, N_i, and N. For the parameters used in Figs. 1 and 2, one gets $\varepsilon_F = 5.4$ meV and $M''(\omega=0) = 1.7\times10^{-3}$ meV.

For small, but finite ω $[M'(\omega), M''(\omega) \ll \omega \ll \omega_0]$, I get with Eq. (14) $M'(\omega) \propto \omega M''(0)$ and $M''(\omega) = M''(0)[1+O(\omega^5)]$. The conductivity is written as $\sigma'(\omega) = Ne^2 M''(0)/(m_\sigma \omega^2)$ with an effective mass m_σ given by

$$\frac{m_\sigma}{m} = \left[1 + k_F\alpha \frac{M''(0)}{\varepsilon_F} \right]^2 \sim 1 + \frac{N_i}{g_v N} \frac{1}{(2k_F\alpha)^2} . \tag{23}$$

We shall see in Sec. IV that the mass renormalization due to reactive effects is also an important concept for plasmon-resonance and cyclotron-resonance experiments.

C. The electron-hole contribution to the conductivity

With Eq. (12), one gets for $\delta = 1/b = 0$ the relaxation rate for large frequencies due to the particle-hole decay channel:

$$M''(\omega \gg 2\varepsilon_F) = 64 g_v^2 M''(0)(k_F\alpha) \left[\frac{\alpha}{a^*} \right]^2 \left[\frac{\varepsilon_F}{\omega} \right] \times \exp[-(20 g_v \alpha/a^*)^{1/2} (\omega\varepsilon_F/\omega_0^2)^{1/2}] . \tag{24}$$

Equation (24) clearly demonstrates that for large frequencies the particle-hole channel gives a larger scattering rate than the plasmon channel with $M_p''(\omega) \propto |\omega|^5 \exp(-B\omega^2)$. The conductivity for high frequencies follows the law $\sigma(\omega \gg 2\varepsilon_F) \propto \exp[-2k_F\alpha(\omega/\varepsilon_F)^{1/2}]/\omega^3$.

IV. RESULTS FOR $1/b > 0$ AND $\delta > 0$

In this section, I discuss the random potential with $1/b > 0$ and $\delta > 0$. Only results for $M''(\omega)$ are given.

A. Finite width of the electron gas

In my calculations in Sec. III, I neglected the finite-extension effects of the electron gas perpendicular to the interface [described by the extension parameter $1/b$ (Ref. 1)]. With Eq. (1) (but $\delta=0$), one gets

$$M_p''(\Omega, b) \propto \frac{1}{(1+\Omega^2/2\alpha b)^6} |\Omega|^5 e^{-\Omega^2} . \tag{25}$$

It is easy to derive the frequency $\omega_0(b)$ where $M''(\omega)$ has a maximum:

$$\omega_0(b) = \omega_0(\tfrac{7}{10})^{1/2} [(1 + \tfrac{136}{49}\alpha b + \tfrac{16}{49}\alpha^2 b^2)^{1/2} - 1 - \tfrac{4}{7}\alpha b]^{1/2} . \tag{26}$$

Asymptotic expressions are given by

$$\omega_0(b) = \omega_0 \left[1 - \frac{3}{2\alpha b} \right] \quad \text{for } \alpha b \gg 1 \tag{27a}$$

and

$$\omega_0(b) = \omega_0(\tfrac{4}{7}\alpha b)^{1/2} = 2\varepsilon_F \frac{1}{k_F a^*} (\tfrac{5}{7} g_v a^* b)^{1/2} \quad \text{for } \alpha = 0 . \tag{27b}$$

For $\alpha=0$, I get

$$M''(\Omega, b) = M''(\omega=0, b) \left[1 + \frac{\pi}{32 g_v^2} (k_F a^*)^2 (1 + g_v k_F a^*)^2 \left[\frac{\omega}{\varepsilon_F} \right]^5 \frac{(1+2k_F/b)^6}{(1+\Omega^2/2\alpha b)^6} \right] \tag{28a}$$

and[21]

$$M''(\omega=0,\, b)=\varepsilon_F \frac{\pi}{g_v}\frac{N_i}{N}\frac{1}{(1+g_v k_F a^*)^2}\frac{1}{(1+2k_F/b)^6}\ . \tag{28b}$$

For $k_F a^* \ll 1$, one finds with Eqs. (27b) and (28)

$$M_p''(\omega_0(b))/M''(\omega=0,\, b)=0.053\left[\frac{g_v}{k_F a^*}\right]^{1/2}\times\left[\frac{b}{k_F}\right]^{5/2}\left[1+\frac{2k_F}{b}\right]^6 . \tag{29}$$

The enhancement factor depends on the electron density via k_F and increases for decreasing N. However, for small electron densities multiple-scattering effects (which lead to a reduction of the enhancement) become important, see Refs. 9 and 10.

In Fig. 3, I plotted $\omega_0(b)$ versus α according to Eq. (26) for $N=1.5\times10^{11}$ cm^{-2} and $N_D=5\times10^{10}$ cm^{-2}. The finite-extension effects reduce the frequency where $M''(\omega)$ has a maximum. But for $\alpha/a^*>1$, the corrections due to the finite-extension effects are small, see Eq. (27a).

For the derivation of Eqs. (25)–(29), I have neglected the finite-extension effects on the electron-electron interaction potential which enter Eq. (8). Neglecting the image potential, the electron-electron interaction potential is expressed as

$$V(q)=2\pi e^2 F(q)/(\epsilon_L q)$$

and

$$F(q)=[1+9q/(8b)+3q^2/(8b^2)]/(1+q/b)^3 =1-15q/(8b)+O(q^2)$$

is the form factor for the finite width. If I include the finite-width effects of the electron-electron interaction and the electron-impurity interaction for the calculation of the maximum of $M''(\omega)$, I get the following asymptotic expressions:

$$\omega_0(b)=\omega_0\left[1-\frac{33}{32\alpha b}\right]\quad \text{for } \alpha b\gg 1 \tag{30a}$$

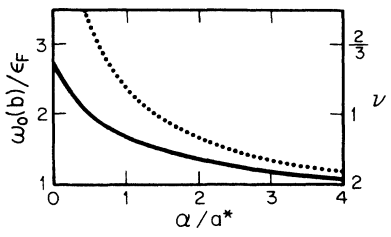

FIG. 3. $\omega_0(b)$ vs α for $N=1.5\times10^{11}$ cm^{-2} and $N_D=5\times10^{10}$ cm^{-2} according to Eq. (26). The dotted line corresponds to $1/b=0$, see Eq. (16). ν is the Landau filling factor defined by $\nu=2\varepsilon_F/\omega_0(b)$ ($g_v=1$).

and

$$\omega_0(b)=2\varepsilon_F\frac{1}{k_F a^*}(1.22 g_v a^* b)^{1/2}\quad \text{for } \alpha=0\ . \tag{30b}$$

By comparing Eq. (27a) with Eq. (30a), one finds that the finite-width effects of the electron-electron interaction compensate in part for the width effects of the electron-impurity interaction. Equation (30) should be helpful for silicon MOS structures because one expects that most of the impurities are located at or near the Si/SiO$_2$ interface ($\alpha=0$). However, my analytical results for $\alpha=0$ [Eqs. (28) and (29)] are not as accurate as the results for $\alpha/a^*\gg1$ [Eqs. (14b) and (17a)] because I neglected the width effects on the electron-electron interaction potential in order to get transparent analytical results.

B. Finite width of doping

In Sec. III, the finite width δ of the remote doping was set to $\delta=0$. With Eq. (1) (but with $1/b=0$), one gets for $\delta>0$

$$M_p''(\Omega)\propto|\Omega|^3 e^{-\Omega^2}(1-e^{-\Omega^2\delta/\alpha})\ . \tag{31}$$

One derives the following asymptotic expressions:

$$\omega_0(\delta)=\omega_0\left[1-\frac{\delta}{4\alpha}+O(\delta^2)\right]\quad \text{for } \delta/\alpha\ll1 \tag{32a}$$

and

$$\omega_0(\delta)=\omega_0(\tfrac{3}{5})^{1/2}\quad \text{for } 1/\delta=0\ . \tag{32b}$$

In Fig. 4, I show $\omega_0(\delta)$ versus δ. A finite doping width reduces the frequency ω_0 where $M''(\omega)$ has a maximum.

For $\delta>\alpha$, it is favorable to introduce a three-dimensional doping density $N_B=N_i/\delta$. The inverse relaxation time for zero frequency and large spacer width is expressed as

$$M''(\omega=0,\,\delta)=\varepsilon_F\frac{1}{4g_v}\frac{N_B}{Nk_F}\frac{1}{(2k_F\alpha)^2}\left[1-\frac{1}{(1+\delta/\alpha)^2}\right], \tag{33}$$

and the enhancement factor is given by

$$M_p''(\omega_0(1/\delta=0))/M''(\omega=0,\,1/\delta=0)=3.64\left[g_v\frac{\alpha}{a^*}\right]^{1/2}. \tag{34}$$

Comparing Eq. (17a) with Eq. (34), I conclude that a finite doping width only slightly changes the enhancement factor. However, $\omega_0(\delta)$ depends on δ, see Fig. 4.

C. High-frequency conductivity

For $1/b=0$ and $1/\delta=0$ one derives with Eq. (12)

$$M''(\omega\gg2\varepsilon_F)=64 g_v^2 M''(\omega=0,\,1/\delta=0)\left[\frac{\alpha}{a^*}\right]^2\times\left[\frac{\varepsilon_F}{\omega}\right]^{3/2}\exp\left[-2k_F\alpha\left[\frac{\omega}{\varepsilon_F}\right]^{1/2}\right], \tag{35}$$

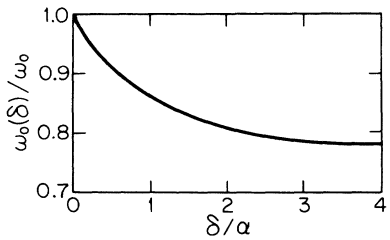

FIG. 4. $\omega_0(\delta)$ vs δ calculated with Eq. (31). ω_0 is given in Eq. (16).

and $M(\omega=0, 1/\delta=0)$ is given in Eq. (33). The high-frequency conductivity is expressed as $\sigma(\omega \gg 2\varepsilon_F) \propto \exp[-2k_F\alpha(\omega/\varepsilon_F)^{1/2}]/\omega^{7/2}$.

For $\alpha=0$ and $\delta=0$, one gets

$$M''(\omega \gg 2\varepsilon_F)=8g_v\varepsilon_F\frac{N_i}{N}\frac{1}{(a^*k_F)^2}\frac{\varepsilon_F}{\omega} \times\frac{1}{[1+(\omega/\varepsilon_F)^{1/2}k_F/b]^6} . \quad (36)$$

The high-frequency conductivity follows the law $\sigma(\omega \gg 2\varepsilon_F) \propto 1/\omega^6$. Because of the low absolute value of the conductivity at large frequencies, it will be very difficult to measure the asymptotic laws given in Eqs. (35) and (36).

V. RESULTS FOR OTHER SCATTERING MECHANISMS

In this section, I calculate the effect of an additional scattering mechanism on the enhancement factor and present results for interface-roughness scattering.

A. Enhancement factor

The conductivity of $Al_xGa_{1-x}As/GaAs$ heterostructures with large spacer width is usually lower than expected theoretically. This is because additional scattering mechanisms (scattering by background impurities, interface-roughness scattering, and alloy-disorder scattering) are present.

For simplicity, let us assume that the additional scattering mechanism has a negligible frequency dependence in the frequency range $\omega_1<\omega<\omega_2$: $M_2(\omega)=M_2(0)$. Then, the characteristic frequencies ω_0 and ω^* are determined by $M_1(\omega)$. However, the enhancement factor of the relaxation rate is reduced by the presence of the second scattering mechanism, and the total inverse scattering time is written as

$$M''(\omega)=[M_1''(0)+M_2''(0)]\left[1+\frac{M_{p1}''(\omega)/M_1''(0)}{1+M_2''(0)/M_1''(0)}\right] . \quad (37)$$

The factor $1/[1+M_2''(0)/M_1''(0)]$ in Eq. (37) describes this reduction of the enhancement factor, compare with Eq. (17a).

Of course, my assumption of a non-frequency-dependent scattering time is somehow artificial. The frequency dependence of the scattering time for interface-roughness scattering was discussed in Ref. 10. Homogeneous background doping was considered in Ref. 22.

B. Interface-roughness scattering

The random potential for interface-roughness scattering is written as[1]

$$\langle|U(\mathbf{q})|^2\rangle=\pi[2g_v\Delta\Lambda\varepsilon_F(1+2N_D/N)/a^*]^2e^{-(q\Lambda/2)^2} , \quad (38)$$

and Λ and Δ are the length parameters of the roughness. One gets for a long-range interface-roughness scattering ($\Lambda b \gg 2$ and $\Lambda \gg a^*$)

$$M''(\Omega)=M''(\omega=0,\Lambda)\left[1+\frac{1}{96}\left[g_v\frac{\pi\Lambda}{2a^*}\right]^{1/2}\left[\frac{\Lambda}{\alpha}\right]^{9/2} \times|\Omega|^9e^{-\Omega^4\Lambda^2/(16\alpha^2)}\right] \quad (39a)$$

and[21]

$$M''(\omega=0,\Lambda)=3\pi^{1/2}\varepsilon_F\frac{1}{k_F\Lambda}\frac{\Delta^2}{\Lambda^2}\left[1+2\frac{N_D}{N}\right]^2 . \quad (39b)$$

I derive with Eq. (39a) for $\Lambda b \gg 2$ and $\Lambda \gg a^*$

$$\omega_0(\Lambda)=2\varepsilon_F\left[\frac{3g_v}{\Lambda a^*k_F^2}\right]^{1/2}\propto\varepsilon_F^{1/2} , \quad (39c)$$

and the enhancement factor is written as

$$M_p''(\omega_0(\Lambda))/M''(\omega=0,\Lambda)=4.37\left[g_v\frac{\Lambda}{a^*}\right]^{1/2} . \quad (39d)$$

The enhancement factor for long-range interface-roughness scattering is similar to the enhancement factor for long-range Coulomb scattering, compare Eq. (39d) with Eq. (17a).

For short-range interface-roughness scattering, one derives $M_p''(\omega)\propto|\omega|^9/(1+C_2\omega^2)^6$ with $C_2\omega^2=\Omega^2/(2\alpha b)$ and

$$\omega_0(\Lambda)=2\varepsilon_F\left[\frac{3g_vb}{k_F}\right]^{1/2}\propto\varepsilon_F^{3/4} \text{ for } \Lambda b \ll 2 . \quad (40)$$

VI. PLASMON AND CYCLOTRON RESONANCE

In this section, I discuss the implications of the frequency-dependent scattering time on plasmon-excitation and cyclotron-resonance experiments. I present results for $\delta=1/b=0$.

A. Plasmon resonance

The Drude conductivity can be considered as a resonance phenomenon with resonance frequency $\omega_R=0$ and half-width at half maximum (HWHM) $\Sigma_\sigma=M''(0)$. The high-frequency conductivity is small, and the peak in $M''(\omega)$ is difficult to measure in experiments. Grating couplers[7,14,15] make it possible to study plasmons in a resonance experiment with resonance frequency $\omega_R=\omega_{p0}(q)$. It was shown before[9] that in the presence of

weak disorder the plasmon energy is shifted to $\omega_{pr}=\omega_{p0}-M'(\omega_{p0})/2$ and the HWHM is given by $\Sigma_p=M''(\omega_{p0})/2$. With $\omega_{pr}^2\propto 1/m_p$, I define a plasmon mass m_p and get for $M'(\omega_{p0}),M''(\omega_{p0})\ll\omega_{p0}\ll\omega_0$

$$\frac{m}{m_p}=\left[1-\tfrac{1}{2}k_F\alpha\frac{M''(0)}{\varepsilon_F}\right]^2\sim\left[\frac{m}{m_\sigma}\right]^{1/2}. \tag{41}$$

Equation (41) demonstrates that for weak disorder the plasmon mass is determined by $M'(\omega)\propto\omega M''(0)$. For a non-frequency-dependent scattering rate, the plasmon mass would be determined by $M''(0)$.[2,23] However, my results show explicitly that a non-frequency-dependent scattering time and the concept of an interacting-electron gas with plasmons is inconsistent. For strong disorder $M''(\omega)$ will also contribute to the plasmon mass.[9]

For $\omega=\omega_{p0}$, one gets with Eq. (14)

$$M'(\omega_{p0})=M''(\omega=0)2\left[g_v\frac{\alpha}{a^*}q\alpha\right]^{1/2}\times[1+2q\alpha-4q^2\alpha^2\mathrm{Ei}(2q\alpha)e^{-2q\alpha}] \tag{42a}$$

and

$$M''(\omega_{p0})=M''(\omega=0)\left[1+8\pi\left[g_v\frac{\alpha}{a^*}(q\alpha)^5\right]^{1/2}e^{-2q\alpha}\right]. \tag{42b}$$

$M'(\omega_{p0})$ and $M''(\omega_{p0})$ describe the shift and the width of the resonance, respectively. The peak structure in $M''(\omega)$ gives rise to a maximum linewidth of plasmons with $\omega_{p0}=\omega_0$. With Eqs. (2), (14), and (16), I predict that plasmons with wave number $q=q_0$, and

$$q_0\alpha=\tfrac{5}{4}, \tag{43}$$

have maximum linewidth. For $1/b=1/\delta=0$ and $\alpha/a^*\gg1$, I get $q_0\alpha=\frac{3}{4}$. With Eq. (27b), I derive, for $\alpha=\delta=0$ and $1/b>0$, $q_0/b=\frac{5}{7}$. Because of the frequency dependence of $M'(\omega)$, I expect the following relations to hold: $\omega_{pr}<\omega_{p0}$ ($\omega_{pr}>\omega_{p0}$) for $\omega_{p0}<\omega^*$ ($\omega_{p0}>\omega^*$). The disorder-induced energy shift of the plasmon might be interpreted as an effective plasmon mass, see Ref. 7.

B. Cyclotron resonance

For finite magnetic field the cyclotron frequency ω_c is the resonance frequency and the high-frequency conductivity can be studied easily. However, the magnetic field will also modify $M'(\omega)$ and $M''(\omega)$. I have successfully analyzed[10,11] some experimental results on cyclotron-resonance anomalies found in silicon MOS systems and $Al_xGa_{1-x}As/GaAs$ heterostructures under the assumption that $M'(\omega)$ and $M''(\omega)$ are not modified by the magnetic field.[1] With an argument which neglected quantum effects, I estimated that this approximation should be applicable for $\nu\gg k_Fa^*$.[11] $\nu=2\pi Nl_0^2$ is the filling factor of the Landau levels, and l_0 is the magnetic length.

Again, as for plasmons, one expects a disorder-induced shift of the resonance energy $\omega_{cr}=\omega_c-M'(\omega_c)$ and a HWHM $\Sigma_c=M''(\omega_c)$.[10,11] I use $\omega_{cr}\propto1/m_c$ for the definition of a effective cyclotron-resonance mass m_c and derive for $M'(\omega_c),M''(\omega_c)\ll\omega_c\ll\omega_0$

$$\frac{m}{m_c}=1-k_F\alpha\frac{M''(0)}{\varepsilon_F}\sim\left[\frac{m}{m_\sigma}\right]^{1/2}. \tag{44}$$

The peak structure in $M''(\omega)$ gives rise to a maximum linewidth for $\omega_c=\omega_0$. This frequency corresponds to the Landau filling factor ν_0 ($\omega_c/\varepsilon_F=2g_v/\nu$) given by

$$\nu_0=\left[\frac{8\pi}{5}Na^*\alpha\right]^{1/2}. \tag{45}$$

The filling factor is indicated in Figs. 1 and 2, and the linewidth maximum is found for $\nu\sim2.4$.

VII. DISCUSSION

A. Range of validity

For small wave numbers the plasmon dispersion $\omega_p(q)$ is given by[1,11] $\omega_p(q)=\omega_{p0}(q)[1+3qa^*/(8g_v)-q/(4g_vk_F)-15q/(8b)+O(q^2)]$. In Eq. (2), I neglected the higher-order terms and only took into account $\omega_{p0}(q)$. Therefore, the validity conditions for Eq. (2) are $qa^*\ll8g_v/3$, $q/k_F\ll4g_v$, and $q\ll8b/15$.

For a doping model with finite spacer only $0<q<1/2\alpha$ are important for the q integral in Eq. (6) resulting in the following validity conditions for Eq. (6): $a^*/\alpha\ll16g_v/3$ and $k_F\alpha\gg8g_v$. For $\alpha=0$, the range of the q integral is determined by $q<b/6$, resulting in $ba^*\ll16g_v$ and $k_F/b\gg1/(24g_v)$ as the validity conditions for Eq. (6).

The calculations are performed in the lowest order of the electron-impurity coupling ($\sim N_i$). Therefore, the impurity density should be low so that multiple-scattering effects can be neglected, see Refs. 9–11. I mention that the static transport properties in the case of a large spacer width are determined by a long-range random potential.[18]

My calculation on the plasmon contribution to the scattering rate is not restricted in the frequency range if Landau damping (the decay of plasmons into electron-hole excitations) is neglected. Landau damping becomes possible for $q\geq q_L$,[6] and q_L is expressed in

$$q_La^*=2g_v[(1+2k_F/q_L)^{1/2}-1][1-G(q_L)]F(q_L). \tag{46}$$

$G(q)$ describes local-field corrections.[6] Plasmons as defined in Eq. (2) are only well defined for $\omega<\omega_L=\omega_{p0}(q=q_L)$. If I assume that $2k_F/q_L\gg1$, I find $q_La^*=2g_v(k_Fa^*/g_v)^{1/3}$. With Eq. (2), I get

$$\omega_L=\omega_0\left[\tfrac{8}{5}g_v\frac{\alpha}{a^*}\right]^{1/2}\left[\frac{k_Fa^*}{g_v}\right]^{1/6}\ggg(\tfrac{3}{5})^{1/2}\omega_0. \tag{47}$$

From Eq. (47), I conclude that Landau damping can be neglected for the description of the peak structure in $M''(\omega)$.

The results for the electron-hole contribution represent expansions for small and large frequencies. For large spacer width, the plasmon contribution is much larger

than the electron-hole contribution to the scattering rate, and it is sufficient to consider only the plasmon contribution.

The energy shift and the width of the plasmon have been calculated within the hydrodynamic approximation of the density-density relaxation function.[9] This approximation is valid at the plasmon energy for $q \ll g_v/a^*$. For $q=q_0=5/(4\alpha)$, one gets $\alpha/a^* \gg 5/(4g_v)$.

B. Relation to other work

In this paper, I have shown (by giving analytical results) that for a long-range random potential the plasmon anomalies are strongly enhanced and the enhancement factor is given by $M_p''(\omega_0)/M''(\omega=0)=3.60(g_v\alpha/a^*)^{1/2}$. The enhancement factor is nonanalytical in the spacer width.

For a long-range random potential the scattering time $\tau_t^{-1}=M''(\omega=0)$ is strongly enhanced due to the reduced backscattering.[18] Backscattering is less reduced for the single-particle relaxation time τ_s, which determines the density of states (the Green's function), and one expects that $\tau_t/\tau_s \gg 1$, which was shown numerically in Refs. 24 and 25. For $2k_F\alpha \gg 1$, one can derive the analytical result:[26]

$$\tau_t/\tau_s=(2k_F\alpha)^2 . \tag{48}$$

In Eq. (43), I predicted a maximum linewidth for plasmons with $q\alpha=\frac{5}{4}$. If one defines a plasmon scattering time τ_p by $1/[\tau_p(\omega_{p0})]=M''(\omega_{p0})$, one gets for $q\alpha=\frac{5}{4}$ ($\omega_{p0}=\omega_0$)

$$\tau_t/\tau_p(\omega_0)=1+3.60\left[g_v\frac{\alpha}{a^*}\right]^{1/2} . \tag{49a}$$

A similar result holds for long-range interface-roughness scattering (replace α by Λ and 3.60 by 4.37). The nonanalytical enhancement of the scattering rate seems to be a general property of long-range random potentials. For $\omega_{p0} \ll \omega_0$ ($q \ll q_0$), one finds

$$\tau_t/\tau_p(\omega_{p0} \ll \omega_0)=1+8\pi\left[g_v\frac{\alpha}{a^*}\right]^{1/2}(q\alpha)^{5/2} . \tag{49b}$$

The strong reduction of the plasmon scattering time makes it very difficult to relate the linewidth for plasmons (with $\omega_{p0}\sim\omega_0$) to the scattering time at zero frequency. However, the analytical results given in this paper will make it easy to compare my predictions with experimental results. The enhanced contribution of the plasmon dynamics to the scattering rate for a long-range random potential shows that for two-dimensional systems realistic random potentials have to be used in the calculations to get reliable results. Model calculations with $\alpha=1/b=0$ are of little relevance in connection to experiments. My calculations also show that for a realistic random potential, simple analytical results can be derived.

The frequency-dependent scattering rate for impurities at the interface ($\alpha=\delta=0$) and for an ideally two-dimensional electron gas ($1/b=0$) was calculated in Ref. 27. Numerical results have been presented. A very small enhancement factor of 0.3 was reported.[27] The small enhancement factor is presumably due to the high electron density used in Ref. 27.

A generalization of the previous work on plasmon dynamics[9–11,27] was proposed in Ref. 28 for $1/b=0$. Numerical results have been presented for $\alpha=0$. There, a wave-number-dependent current relaxation kernel $M(\omega,q)$ was introduced into the theory. A long time ago it was shown that such a q dependence introduces an artificial singularity into the conductivity at zero frequency for a non-interacting-electron gas in two dimensions[29] if a self-consistent calculation of $M(\omega,q)$ is performed. It is easy to see that an equivalent singularity is present for an interacting-electron gas, and therefore the approach given in Ref. 28 cannot be generalized to include multiple-scattering effects. I want to stress that without this generalization, the results given in Ref. 28 are identical to former results for two dimensions[9–11,27] and three dimensions.[17,30]

If I take into account the q dependence of the current relaxation kernel as in Ref. 28, I get the following analytical results for small q:

$$M''(\omega,q)=M''(\omega=0,q)+M_p''(\omega,q) \tag{50a}$$

with

$$M''(\omega=0,q)=M''(\omega=0)[1+(q\alpha)^2/4+O(q^4)] , \tag{50b}$$

$$M_p''(\omega,q)=M_p''(\omega)\left[1+\tfrac{3}{2}(\alpha q)^2\left[1-\frac{5}{3\Omega^2}\right]+O(q^4)\right] , \tag{50c}$$

and

$$M_p''(\omega)=M''(\omega=0)\pi\left[2g_v\frac{\alpha}{a^*}\right]^{1/2}|\Omega|^5 e^{-\Omega^2} , \tag{50d}$$

see Eq. (14b). For $\omega=\omega_{p0}$, one gets

$$M_p''(\omega_{p0},q)=M_p''(\omega_{p0})[1-\tfrac{5}{4}\alpha q(1-\tfrac{6}{5}\alpha q)+O(q^3)] . \tag{51}$$

In agreement with Ref. 28, I find that the essential q dependence of $M''(\omega_{p0},q)$ is due to $M_p''(\omega_{p0})$, see Eq. (49b).

Reference 28 confirmed previous results (see Fig. 12 of Ref. 10) on the density dependence of the ratio $\tau_t/\tau_p(\omega_{p0})$. In Ref. 28, it was claimed that the ratio $\tau_t/\tau_p(\omega_{p0})$ is nearly independent of α. This result is in contradiction to the results presented in this paper, see Eqs. (42) and (49). It was shown in Ref. 11 that even for $\alpha>0$ the plasmon contribution for small frequencies is independent of α and given by $M_p''(\omega)\propto\omega^5$.[9] $M''(\omega=0)$ depends strongly on α and $\tau_t/\tau_p(\omega_{p0})$ must depend strongly on α, see Eq. (49b).

My results for the cyclotron-resonance anomalies could be criticized because I neglected the magnetic field dependence of the scattering rate. Due to the disorder the Landau levels are broadened, and for low magnetic fields the overlap of the Landau bands will result in a

weak magnetic field dependence of the density of states.[31–33] In my theory, I have used the plasmon dispersion instead of the magnetoplasmon dispersion: $\omega_c(q)=(\omega_c^2+\omega_p^2)^{1/2}$. However, for large q and small magnetic fields the magnetoplasmon dispersion can be approximated by the plasmon dispersion. Small q have only a small weight to the integral in Eq. (6), and therefore my approximation is presumably useful for small magnetic fields. I neglected the magnetic field dependence of the collective modes. Therefore, my theory is certainly wrong for high magnetic fields. It is clear that my theory cannot account for oscillations of the linewidth with the filling factor of the Landau levels as found in Refs. 34 and 35. In this case the filling-factor dependence of the screening due to the oscillating density of states[36,37] is probably a better description.

The importance of disorder for the cyclotron anomalies was pointed out long ago.[38] The calculation in Ref. 38 has been performed for a noninteracting electron gas and can explain positive shifts of the cyclotron resonance. I believe that for large disorder, the relevant physics is included in the approach given in Ref. 38. Apparently,[1] this model cannot explain negative shifts of the cyclotron resonance as seen in experiment.

Anyway, the comparison of theoretical results (where approximations are always necessary) with experimental results can give some hints as to which approximations are tolerable. Therefore, I leave it up to the experimentalists whether they can use my results to understand their experiments.

VIII. COMPARISON WITH EXPERIMENTS

In this section, I discuss some plasmon-excitation experiments and compare some cyclotron-resonance experiments with theory.

A. Plasmon-excitation experiments

In Sec. VI, I found that the plasmons with $q\alpha=\frac{5}{4}$ (for $1/b=\delta=0$) have maximal linewidth. The experimental results for plasmon excitation by light[12,39,40] or via a grating coupler[14,15] indicate that $q\alpha=\frac{5}{4}$ is achievable. In Table I some typical parameters of the experiments (q) and the used structures (α,δ) are given.

The largest q value achieved with a grating coupler was reported in Ref. 15: $q=2.0\times10^5$ cm^{-1}. However, in Ref. 15, only a moderate enhancement factor of 0.5 for $q=1.0\times10^5$ cm^{-1} was reported. This is probably due to the small spacer width of this sample, see Eq. (49b). With a similar structure but a larger spacer, the maximum linewidth should be observable using the grating-coupler technique.

An enhancement factor of 3 was reported in Ref. 39 and the reduced-plasmon scattering time was interpreted as the single-particle relaxation time. This interpretation is presumably wrong. The enhanced scattering rate comes from the frequency dependence of $M''(\omega)$ due to plasmon dynamics.[9–11] In Ref. 39 a non-frequency-dependent scattering rate was used for the interpretation of the experiments, and consequently $M'(\omega)=0$ was used. With Eq. (21), I conclude that the change of $M'(\omega)$ is of the same order as the change of $M''(\omega)$. Therefore, I believe that for an enhancement factor of 3 for the scattering rate, as reported in Ref. 39, one should not neglect $M'(\omega)$.

Very large q values have been achieved in Raman spectroscopy experiments:[40] $q<6.8\times10^5$ cm^{-1}. However, in Ref. 40 systematic results on the HWHM have not been reported.

From the analysis of the experiments, I conclude that with the presently available technology, one should observe the frequency-dependent scattering time and that one could reach the maximum at $q\alpha=\frac{5}{4}$. However, one should use samples with a well-known scattering mechanism (determinable from the density dependence of the mobility) to get interpretable results.

In the experiments on silicon MOS systems[7] it was found that $\omega_{pr}<\omega_{p0}$ ($m_p>m$). I predict that for larger q and for cleaner samples also $\omega_{pr}>\omega_{p0}$ ($m_p<m$) could be measured in experiment. This will happen for $\omega_{p0}>\omega^*$. With $Al_xGa_{1-x}As/GaAs$ heterostructures it is probably easier to reduce the disorder and to reach the weak disorder limit.

B. Cyclotron-resonance experiments

In a very recent paper[41] on cyclotron-resonance anomalies in $Al_xGa_{1-x}As/GaAs$ heterostructures it was claimed that the cyclotron-resonance anomalies found in silicon MOS systems are by common consent due to imperfections. I claim that there exists no consensus on the origin of these anomalies, see Refs. 3–5. The argument that the cyclotron-resonance anomalies are due to the frequency-dependent scattering time (disorder) was originally put forward in Refs. 10 and 11 on the basis of a comparison of experiments with theory. In the analyzed experiments[42] sodium ions have been drifted to the SiO_2/Si interface, resulting in a well-defined scattering mechanism. This is in contradiction to the claim in Ref. 41 that the disorder is unspecified in silicon MOS structures.

TABLE I. Typical parameters for plasmon-excitation experiments.

Ref.	Spacer α (Å)	Doping width δ (Å)	q (cm^{-1})	$q\alpha$	$q(\alpha+\delta)$
12	100	200	8×10^4	0.08	0.24
14	50	600	5×10^4	0.03	0.33
15	35	530	20×10^4	0.08	1.14
39	50	250	15×10^4	0.09	0.38
40	200	100	60×10^4	1.20	1.80

In recent cyclotron-resonance experiments on $Al_xGa_{1-x}As/GaAs$ heterostructures[5,16,43] similar anomalies as in silicon MOS systems[2,3] have been reported. A maximum linewidth was found at a certain magnetic field (if the frequency-dependent conductivity is measured) which corresponds to a certain cyclotron frequency. The dependence of this maximum linewidth on the electron density[5,43] and on the spacer width[16] was studied. I have compared ω_0 which depends on N and α [see Eq. (16)] with the experimental results,[5,16] and I find very good agreement, see Table II. The calculated enhancement factors for the inverse scattering rate are larger than found in experiment. This is probably due to an additional scattering mechanism, see Eq. (37).

From Eq. (16), one could conclude that $\omega_0 \propto (N/\alpha)^{1/2}$, which is apparently in agreement with the experimental results of Ref. 43. However, on ungated $Al_xGa_{1-x}As/GaAs$ heterostructures, one finds that $N \propto 1/\alpha$.[44,45] From the theoretical results of Ref. 45 the following relation can be derived:

$$\alpha a^* N \sim \begin{cases} 0.6 & \text{for } x=0.2 \\ 1.2 & \text{for } x=0.3 \\ 1.8 & \text{for } x=0.4 \, . \end{cases} \tag{52}$$

With Eqs. (16) and (52) one now would conclude that $\omega_0 \propto N$, which is in disagreement with the experimental results.[43] However, in the experiments[43] the spacer width in most samples was low (50 Å $< \alpha <$ 400 Å) and the width of the remote doping was large ($\delta = 500$ Å). If one takes into account the width effects via

$$\omega_0(b,\delta) = \omega_0(\delta)\left[1-\frac{3}{2\alpha b}\right] \tag{53}$$

we get good agreement between theory and experiment,[43] see Fig. 5. For Fig. 5, I used $\alpha a^* N = 0.64$.[44] I guess that the splitting of the line found in Ref. 43 is due to a strongly frequency-dependent scattering rate for $\omega_c \sim \omega_0(b,\delta)$ superimposed on a nearly frequency-independent scattering rate. However, I mention that also an inhomogeneous impurity distribution could give rise to a effective long-range potential and to a strongly peaked frequency-dependent scattering time.

The relation between N and α as given in Eq. (52) is for structures without a gate. If one uses Eqs. (45) and (52), one gets

$$\nu_0 \approx \begin{cases} 1.7 & \text{for } x=0.2 \\ 2.5 & \text{for } x=0.3 \\ 3.0 & \text{for } x=0.4 \, . \end{cases} \tag{54}$$

Equation (54) might explain why in experiments with ungated samples and $x \sim 0.25$ often a maximum linewidth of the cyclotron resonance near $\nu \sim 2$ was reported.[46–48] It should be possible to test Eq. (54) in experiment.

For very low filling factors ($\nu < 0.5$) a linewidth narrowing is found in some cyclotron-resonance experiments.[3,49] Low filling factors correspond to high frequencies, and my condition $\omega \gg 2\varepsilon_F$ for the high-frequency conductivity corresponds to $\nu \ll g_v$. My results on the high-frequency conductivity indicate that $M''(\omega \gg 2\varepsilon_F)/M''(\omega=0) \ll 1$. This result, if applied to the cyclotron-resonance experiments, could be interpreted as a linewidth narrowing. However, if for fixed magnetic field the electron density is reduced (to get a lower filling factor) one reaches the metal-insulator transition,[11] and the linewidth should increase again. This increase is due to multiple-scattering effects and cannot be described by the present theory, see Refs. 9 and 10. A linewidth narrowing and a following linewidth increase with decreasing filling factor was observed in Ref. 49. I think that my theory is best applied for the large-filling-factor regime and my results on the high-frequency-dependent scattering rate should be applied only with large caution to the cyclotron linewidth narrowing. But my calculation on the high-frequency scattering rate shows that the relation $M''(\omega \gg 2\varepsilon_F)/M''(\omega=0) \ll 1$ is not a surprising result, but occurs already for zero magnetic field.

It is hard to believe that the good agreement between my theory and the experimental results (see Table II and Fig. 5) is accidental. For an explanation of the positive and negative shifts of the cyclotron resonance,[2,3,16,43] one

TABLE II. Comparison of ω_0 from theory ($\omega_0^{(\text{theor})}$) and experiments ($\omega_0^{(\text{expt})}$) for $Al_xGa_{1-x}As/GaAs$ heterostructures. For $\omega_0^{(\text{theor})}$ we used Eq. (16). $\omega_0^{(\text{expt})}$ is taken from experimental results of Refs. 5 and 16.

Ref.	Spacer α (Å)	Density N (cm^{-2})	$\omega_0^{(\text{theor})}$ (cm^{-1})	$\omega_0^{(\text{expt})}$ (cm^{-1})
5	500	8×10^{10}	32	30
5	500	6.5×10^{10}	29	27
5	500	5×10^{10}	26	22
5	500	3.5×10^{10}	21	15
16	750	1.5×10^{11}	35	42
16	750	8×10^{10}	26	23
16	800	8×10^{10}	29	25
16	1600	6×10^{10}	15	17
16	1600	2.5×10^{10}	10	<12
16	3200	5×10^{10}	10	<15

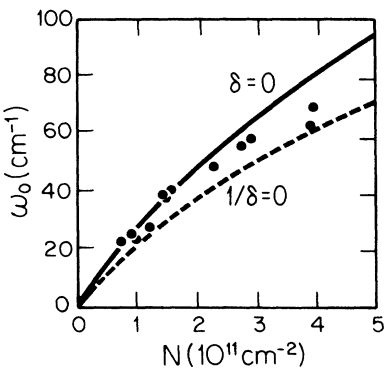

FIG. 5. ω_0 vs electron density according to Eq. (53). The dots are experimental results for the linewidth maximum from Ref. 43.

needs an $M'(\omega)$ which changes sign. For an noninteracting-electron gas in zero magnetic field, one finds that $M'(\omega)<0$ for all frequencies.[18] The inclusion of the plasmon dynamics give rise to a positive M' for $\omega<\omega^*$. Therefore, I believe that the collective modes in an interacting-electron system are essential to understand the cyclotron anomalies. The similarities between my theory on $M'(\omega)$ [and $M''(\omega)$] and the experimental results on $\omega_c-\omega_{cr}$ (and the HWHM) (Refs. 3, 5, and 43) are so striking that according to my opinion the interpretations of the experimental results in terms of a Wigner crystal[3] or of exciton physics[5] is very questionable.

IX. CONCLUSION

The frequency-dependent scattering time of a disordered interacting-electron gas in two dimensions has been calculated. Analytical results for the plasmon contribution to the relaxation rate have been presented for $Al_xGa_{1-x}As/GaAs$ heterostructures with large spacer width.

I have shown that the plasmon decay channel is the dominant channel for the current decay for frequencies $\omega_1<\omega<\omega_2$ and that for a large spacer width the contribution of the plasmon channel to the scattering rate is much larger than the contribution of the particle-hole channel. The frequency-dependent scattering rate (dissipative) implies a reactive part of the current relaxation kernel, which is of the same order of magnitude as the dissipative part. Therefore, the concept of plasmons for the density excitation spectrum implies a frequency-dependent current relaxation kernel for the dynamical conductivity.

The frequency-dependent scattering time determines the linewidth of plasmon excitations, and I predicted a maximum linewidth near $q\alpha=\frac{5}{4}$ $(1/b=\delta=0)$. The comparison of my theory with cyclotron-resonance experiments suggests that the cyclotron-resonance anomalies found in experiments[5,16] are due to a collective mode, and the agreement between my theory (where magnetic field effects on the scattering rate are neglected) and the experiments is surprisingly good, see Table II and Fig. 5.

For high frequencies the electron-hole contribution to the scattering is dominant. I showed that the frequency dependence of the scattering rate strongly depends on the large q dependence of the random potential and $M''(\omega\gg 2\varepsilon_F)\ll M''(\omega=0)$.

The presented analytical results depend on measurable quantities of the two-dimensional electron gas (N,N_D) and the doping profile of the heterostructure (α,δ,N_i). My theory has predictive power and thus can be tested in experiments. This fact could challenge some experimentalists.

ACKNOWLEDGMENTS

I thank P. A. Lee for discussions. This work was supported by the Deutsche Forschungsgemeinschaft (Bonn, Germany) and the U.S. Joint Services Electronics Program (under Contract No. DAAL03-89-C-0001).

[1]T. Ando, A. B. Fowler, and F. Stern, Rev. Mod. Phys. **54**, 437 (1982).

[2]G. Abstreiter, J. P. Kotthaus, J. F. Koch, and G. Dorda, Phys. Rev. B **14**, 2480 (1976); T. A. Kennedy, R. J. Wagner, B. D. McCombe, and D. C. Tsui, Solid State Commun. **22**, 459 (1977); R. J. Wagner, T. A. Kennedy, B. A. McCombe, and D. C. Tsui, Phys. Rev. B **22**, 945 (1980).

[3]B. A. Wilson, S. J. Allen, Jr., and D. C. Tsui, Phys. Rev. B **24**, 5887 (1981), and references cited therein.

[4]I. V. Lerner and Yu. E. Lozovik, Zh. Eksp. Teor. Fiz. **78**, 1167 (1980) [Sov. Phys.—JETP **51**, 588 (1980)]; C. Kallin and B. I. Halperin, Phys. Rev. B **31**, 3635 (1985).

[5]Z. Schlesinger, W. I. Wang, and A. H. MacDonald, Phys. Rev. Lett. **58**, 73 (1987).

[6]D. Pines and P. Nozières, *The Theory of Quantum Liquids* (Benjamin, New York, 1966), Vol. I, Chap. 4.

[7]S. J. Allen, Jr., D. C. Tsui, and R. A. Logan, Phys. Rev. Lett. **38**, 980 (1977); T. N. Theis, J. P. Kotthaus, and P. J. Stiles, Solid State Commun. **24**, 273 (1977); D. Heitmann, J. P. Kotthaus, and E. G. Mohr, Solid State Commun. **44**, 715 (1982); E. Batke and D. Heitmann, *ibid.* **47**, 819 (1983).

[8]A. Gold, W. Götze, C. Mazure, and F. Koch, Solid State Commun. **49**, 1085 (1984); see also J. S. Allen, D. C. Tsui, and F. de Rosa, Phys. Rev. Lett. **35**, 1359 (1975).

[9]A. Gold and W. Götze, Phys. Rev. B **33**, 2495 (1986); see also Solid State Commun. **47**, 627 (1983).

[10]A. Gold, Phys. Rev. B **32**, 4014 (1985).

[11]A. Gold, Z. Phys. B **63**, 1 (1986).

[12]D. Olego, A. Pinczuk, A. C. Gossard, and W. Wiegmann, Phys. Rev. B **26**, 7867 (1982).

[13]R. Höpfel, G. Lindemann, E. Gornik, G. Stangl, A. C. Gossard, and W. Wiegmann, Surf. Sci. **113**, 118 (1982).

[14]E. Batke, D. Heitmann, J. P. Kotthaus, and K. Ploog, Phys. Rev. Lett. **54**, 2367 (1985).

[15]E. Batke, D. Heitmann, and C. W. Tu, Phys. Rev. B **34**, 6951 (1986).

[16]R. J. Nicholas, M. A. Hopkins, D. J. Barnes, M. A. Brummel, H. Sigg, D. Heitmann, K. Ensslin, J. J. Harris, C. T. Foxon, and G. Weimann, Phys. Rev. B **39**, 10955 (1989). Similar results have been published by K. Ensslin, D. Heitmann, H. Sigg, and K. Ploog, Phys. Rev. B **36**, 8177 (1987).

[17]W. Götze and P. Wölfle, Phys. Rev. B **6**, 1226 (1972).

[18]A. Gold and W. Götze, J. Phys. C **14**, 4049 (1981).

[19]P. J. Price, J. Vac. Sci. Technol. **19**, 599 (1981).

[20]I. S. Gradshteyn and I. M. Ryzhik, *Table of Integrals, Series and Products* (Academic, New York, 1980), Chap. 9.

[21]A. Gold and V. T. Dolgopolov, Phys. Rev. B **33**, 1078 (1986).

[22]A. Gold, Phys. Rev. B **35**, 723 (1987).

[23]G. F. Giuliani and J. J. Quinn, Phys. Rev. B **29**, 2321 (1984).

[24]J. P. Harrang, R. J. Higgins, R. K. Goodall, P. R. Jay, M. Laviron, and P. Delescluse, Phys. Rev. B **32**, 8126 (1985).

[25]S. Das Sarma and F. Stern, Phys. Rev. B **32**, 8442 (1985).

[26]A. Gold, Phys. Rev. B **38**, 10798 (1988).

[27]N. Tzoar, P. M. Platzman, and A. Simons, Phys. Rev. Lett.

36, 1200 (1976).
[28]D. Belitz and S. Das Sarma, Phys. Rev. B **34**, 8264 (1986).
[29]D. Vollhardt and P. Wölfle, Phys. Rev. B **22**, 4666 (1980).
[30]A. Gold, Ph.D. thesis, Technical University of Munich, 1984.
[31]E. Gornik, R. Lassnig, G. Strasser, H. L. Störmer, A. C. Gossard, and W. Wiegmann, Phys. Rev. Lett. **54**, 1820 (1985).
[32]J. P. Eisenstein, H. L. Störmer, V. Narayanamurti, A. Y. Cho, A. C. Gossard, and C. W. Tu, Phys. Rev. Lett. **55**, 875 (1985).
[33]S. Das Sarma and X. C. Xie, Phys. Rev. Lett. **61**, 738 (1988).
[34]Th. Englert, J. C. Maan, Ch. Uihlein, D. C. Tsui, and A. C. Gossard, Solid State Commun. **46**, 545 (1983).
[35]D. Heitmann, M. Ziesmann, and L. L. Chang, Phys. Rev. B **34**, 7463 (1986).
[36]R. Lassnig and E. Gornik, Solid State Commun. **47**, 959 (1983).
[37]T. Ando and Y. Murayama, J. Phys. Soc. Jpn. **54**, 1519 (1985).
[38]H. J. Mikeska and H. Schmidt, Z. Phys. B **20**, 43 (1975).
[39]G. Fasol, M. Mestres, A. Fischer, and K. Ploog, Phys. Scr. **T19**, 109 (1987).
[40]T. Egeler, S. Beeck, G. Abstreiter, G. Weimann, and W. Schlapp, Superlat. Microstruct. **5**, 123 (1989).
[41]H. Sigg, D. Weiss, and K. v. Klitzing, Surf. Sci. **196**, 293 (1988).
[42]H. R. Chang and F. Koch, in *Application of High Magnetic Fields in Semiconductor Physics,* Vol. 177 of *Lecture Notes in Physics,* edited by G. Landwehr (Springer-Verlag, Berlin, 1983), p. 127.
[43]Z. Schlesinger, S. J. Allen, J. C. M. Hwang, P. M. Platzman, and N. Tzoar, Phys. Rev. B **30**, 435 (1984).
[44]J. C. M. Hwang, A. Kastalsky, H. L. Störmer, and V. G. Keramidas, Appl. Phys. Lett. **44**, 802 (1984).
[45]T. Ando, J. Phys. Soc. Jpn. **51**, 3900 (1982).
[46]K. Muro, S. Mori, S. Narita, S. Hiyamizu, and K. Nanbu, Surf. Sci. **142**, 394 (1984).
[47]E. Gornik, W. Seidenbusch, R. Lassnig, H. L. Störmer, A. C. Gossard, and W. Wiegmann, in *Two-Dimensional Systems, Heterostructures and Superlattices,* Vol. 53 of *Springer Series in Solid State Sciences,* edited by G. Bauer, F. Kuchar, and H. Heinrichs (Springer-Verlag, Heidelberg, 1984), p. 60; W. Seidenbusch, E. Gornik, and G. Weimann, Phys. Rev. B **36**, 9155 (1987).
[48]E. Batke, H. L. Störmer, A. C. Gossard, and J. H. English, Phys. Rev. B **37**, 3093 (1988).
[49]M. J. Chou, D. C. Tsui, and G. Weimann, Phys. Rev. B **37**, 848 (1988).